# Interpretation of Mass Spectra from Organic Compounds in Aerosol Time-of-Flight Mass Spectrometry

**ARTICLE** *in* ANALYTICAL CHEMISTRY · SEPTEMBER 2000

Impact Factor: 5.64 · DOI: 10.1021/ac9910132 · Source: PubMed



**2 AUTHORS:**

Philip J. Silva
United States Department of Agriculture
**31** PUBLICATIONS **1,301** CITATIONS

SEE PROFILE

Kim Prather
University of California, San Diego
**297** PUBLICATIONS **9,850** CITATIONS

SEE PROFILE

*Anal. Chem.* **2000,** *72,* 3553−3562

# Interpretation of Mass Spectra from Organic Compounds in Aerosol Time-of-Flight Mass Spectrometry

Philip J. Silva and Kimberly A. Prather*

*Department of Chemistry, University of California, Riverside, California 92521*

**Organic compounds containing a variety of functional groups have been analyzed using aerosol time-of-flight mass spectrometry. Both positive and negative laser desorption/ionization mass spectra have been acquired for compounds of relevance to ambient air particulate matter, including polycyclic aromatic hydrocarbons, heterocyclic analogues, aromatic oxygenated compounds such as phenols and acids, aliphatic dicarboxylic acids, and reduced nitrogen species such as amines. In many cases, positive ion mass spectra are similar to those found in libraries for 70-eV electron impact mass spectrometry. However, formation of even-electron molecular ions due to adduct formation also plays a major role in ion formation. Negative ion mass spectra suggest that organic compounds largely disintegrate into carbon cluster fragments ($C_n^-$ and $C_nH^-$). However, information about the heteroatoms present in organic molecules, especially nitrogen and oxygen, is carried dominantly by negative ion spectra, emphasizing the importance of simultaneous analysis of positive and negative ions in atmospheric samples.**

The introduction of a number of real-time single-particle mass spectrometry (RTSPMS) techniques[1−6] offers the potential for analysis of aerosol composition and characterization of processes that have eluded analysis for a variety of reasons. These techniques have shown their utility for analysis of source emissions[7] and ambient analysis of particles in the troposphere.[8−12] In addition, other unique applications have been explored.[13−15] However, the use of these techniques for the analysis of organic compounds in aerosols has been limited because of a lack of knowledge regarding the desorption/ionization and fragmentation processes in the techniques and by the complex mixture of organic species present in atmospheric particles.

There is great potential for applying RTSPMS techniques for the analysis of the organic components of atmospheric aerosols. There is a need for on-line analysis techniques for organics because of the limitations of traditional analytical techniques. Data on the presence of semivolatile organic compounds in aerosols can be lost due to volatilization of the compounds after collection on filter media prior to chemical analysis. In addition, many highly polar compounds cannot be readily analyzed using the available suite of off-line techniques such as gas chromatography.

Previous work using laser microprobe mass analysis (LAMMA), the off-line forerunner to these real-time techniques, has elucidated some aspects of the ionization and fragmentation mechanisms observed using laser desorption/ionization.[16−20] However, to date there has been no investigation of the capability of RTSPMS techniques for analysis of the wide range of compounds known and expected to be present in atmospheric particles. The purpose of this study is to understand and identify potential characteristic ion peaks in the mass spectra of various relevant compounds and compound classes expected to be present in atmospheric particulate matter.

## EXPERIMENTAL SECTION

An aerosol time-of-flight mass spectrometer (ATOFMS) provides size and chemical composition information for individual particles. It operates in a continuous sampling manner, allowing for real-time analysis of particles with high time resolution. The

(1) Noble, C. A.; Prather, K. A. *Environ. Sci. Technol.* **1996**, *30*, 2667−2680.
(2) Hinz, K.-P.; Kaufmann, R.; Spengler, B. *Aerosol Sci. Technol.* **1996**, *24*, 233−242.
(3) Carson, P. G.; Johnston, M. V.; Wexler, A. S. *Rapid Commun. Mass Spectrom.* **1997**, *11*, 993−996.
(4) Yang, M.; Reilly, P. T. A.; Boraas, K. B.; Whitten, W. B.; Ramsey, J. M. *Rapid Commun. Mass Spectrom.* **1996**, *10*, 347−351.
(5) Murphy, D. M.; Thomson, D. S. *Aerosol Sci. Technol.* **1995**, *22*, 237−249.
(6) Kievit, O.; Weiss, M.; Verheijen, P. J. T.; Marijnissen, J. C. M.; Scarlett, B. *Chem. Eng. Commun.* **1996**, *151*, 79−100.
(7) Silva, P. J.; Prather, K. A. *Environ. Sci. Technol.* **1997**, *31*, 3074−3080.
(8) Gard, E. E.; Kleeman, M. J.; Gross, D. S.; Hughes, L. S.; Allen, J. O.; Morrical, B. D.; Fergenson, D. P.; Dienes, T.; Gaelli, M.; Cass, G. R.; Prather, K. A. *Science* **1998**, *279*, 1184−1187.
(9) Liu, D.-Y.; Rutherford, D.; Kinsey, M.; Prather, K. A. *Anal. Chem.* **1997**, *69*, 1808−1814.
(10) Murphy, D. M.; Thomson, D. S. *J. Geophys. Res.* **1997**, *102*, 6353−6368.
(11) Murphy, D. M.; Thomson, D. S. *J. Geophys. Res.* **1997**, *102*, 6341−6352.
(12) Murphy, D. M.; Thomson, D. S.; Mahoney, M. J. *Science* **1998**, *282*, 1664−1669.
(13) Noble, C. A.; Prather, K. A. *Aerosol Sci. Technol.* **1998**, *29*, 294−306.
(14) Middlebrook, A. M.; Thomson, D. S.; Murphy, D. M. *Aerosol Sci. Technol.* **1997**, *27*, 293−307.
(15) Ge, Z.; Wexler, A. S.; Johnston, M. V. *J. Colloid Interface Sci.* **1996**, *183*, 68−77.
(16) Van Vaeck, L.; Claereboudt, J.; De Waele, J.; Esmans, E.; Gijbels, R. *Anal. Chem.* **1985**, *57*, 2944−2951.
(17) Hercules, D. M.; Novak, F. P.; Viswanadham, S. K.; Wilk, Z. A. *Anal. Chim. Acta* **1987**, *195*, 61−71.
(18) Van Vaeck, L.; Bennett, J.; Van Epsen, P.; Schweikert, E.; Gijbels, R.; Adams, F.; Lauwers, W. *Org. Mass Spectrom.* **1989**, *24*, 782−796.
(19) Van Vaeck, L.; Bennett, J.; Van Epsen, P.; Schweikert, E.; Gijbels, R.; Adams, F.; Lauwers, W. *Org. Mass Spectrom.* **1989**, *24*, 797−806.
(20) Van Vaeck, L.; De Waele, J.; Gijbels, R. *Mikrochim. Acta* **1984**, *III*, 237−257.

10.1021/ac9910132 CCC: $19.00 
Published on Web 06/24/2000

instrumental setup has been described in detail previously.[21−23] Particles are introduced into the instrument through a nozzle and undergo a supersonic expansion. The particles are accelerated to a terminal velocity that is proportional to their aerodynamic diameter. The particles then enter a sizing region where they pass through two continuous wave laser beams. Scattering signals are collected as each particle passes through each laser beam. This measures a particle time of flight that can be converted to aerodynamic size with a calibration curve. After being sized, the particle travels to the ion source region of a time-of-flight mass spectrometer. Chemical species in the particle are desorbed/ionized, using the pulsed output from an ultraviolet laser, and separated and detected using a reflectron time-of-flight mass spectrometer equipped with multichannel plates (MCPs) for ion detection.

The experiments described in this paper were performed using the laboratory-based ATOFMS.[1,24] An argon ion laser (488- and 514-nm continuous wave output) was used for the aerodynamic sizing region of the instrument, with size calibrations indicating a lower size limit of 0.3 $\mu$m for these experiments. Laser desorption/ionization of chemical species in the particles was accomplished using a Nd:YAG laser operating at 266 nm. Positive and negative ions were acquired separately by changing the applied voltages for the source and reflectron regions of the time-of-flight mass spectrometer.

Several different particle generation techniques were used. Solid samples were ground into a fine powder and the resulting particles were suspended in a small glass bottle. This sampling apparatus was connected to the inlet of the instrument, resulting in the detection and analysis of large particles up to ~8.0 $\mu$m, depending on the fineness of the suspended powder. Liquid samples were analyzed using a home-built atomizer for generation of particles. A limited number of experiments made use of acid−base reactions in order to form particles of organic salts. In these experiments, gas-phase acids and bases were introduced into the glass bottle and the resulting particles were analyzed by ATOFMS. Mixtures of organic compounds were analyzed both by the suspension of homogeneous powders and using a vibrating orifice aerosol generator (VOAG, TSI model 3450) for creation of particles containing mixtures of more than one chemical species. In all cases, mixtures of 1:1 mole ratios were prepared.

Laser energy for the desorption/ionization laser was varied for each compound between approximately 5 and 40 mJ with a spot size of ~0.75 mm, representing typical values used during acquisition of ambient data. This translates into a laser fluence of approximately $10^8$−$10^9$ W cm$^{-2}$. However, due to inhomogeneities in the laser beam, the actual fluence for desorption/ionization from one shot to another can vary considerably. A minimum of 100 positive and negative ion spectra were acquired for each compound or mixture. Spectra chosen for display represent averages of those acquired using both high ($10^9$ W cm$^{-2}$) and low ($10^8$ W cm$^{-2}$) laser fluence. The terms "low" and "high" are used as relative terms for this experiment; however, it is important to note that ions can be formed at even lower fluences, down to a threshold value of $10^6$ W cm$^{-2}$. The experiments presented in this paper were conducted at the chosen fluences to reproduce and gain insight into mass spectra acquired at typical powers used in previous field studies conducted with ATOFMS. This shows both the parent ion region (important at low laser fluence) and fragments from the compounds (important at high laser fluence). In a number of cases, spectra of pure organic compounds also show peaks due to alkali metals such as sodium and potassium, due to the extremely high sensitivity of ATOFMS to these elements that are present as trace impurities (<1%).

Table 1. Polycyclic Aromatic Hydrocarbons and Oxygenated/Aza Polycyclics Analyzed Using ATOFMS

| compound | MW | CAS registry no. |
|---|---|---|
| naphthalene | 128 | 91-20-3 |
| acenaphthene | 154 | 83-32-9 |
| 1,5-dihydroxynaphthalene | 160 | 83-56-7 |
| fluorene | 166 | 86-73-7 |
| phenanthrene | 178 | 85-01-8 |
| phenanthridine | 179 | 229-87-8 |
| 9-fluorenone | 180 | 486-25-9 |
| perinaphthenone | 180 | 548-39-0 |
| fluoranthene | 202 | 206-44-0 |
| pyrene | 202 | 129-00-0 |
| 2-methylanthraquinone | 208 | 84-54-8 |
| phenanthraquinone | 222 | 84-11-7 |
| chrysene | 228 | 218-01-9 |
| perylene | 252 | 198-55-0 |
| benzo[*ghi*]perylene | 276 | 191-24-2 |
| coronene | 300 | 191-07-1 |

## RESULTS AND DISCUSSION

The compounds chosen for analysis in this study are discussed in several broad categories, including aromatic compounds, polycyclic aromatics, aliphatics, and organic salts. The hydrocarbon compounds were chosen on the basis of previously published work indicating the types of compounds present in atmospheric particles or detected in source emissions experiments. In the case of polar compounds and organic salts, compounds were selected on the basis of what has been hypothesized to be present in the atmospheric aerosol. Several selected compounds (halogen- and phosphorus-containing) were chosen solely to probe the characteristic fragments obtained from compounds containing these elements.

**1. Polycyclic Aromatic Hydrocarbons (PAHs) and Analogues.** The presence of PAHs in atmospheric particulate matter has long been a focus of intensive research. Studies have been performed on PAHs in atmospheric particles more than any other class of organic compounds because of their carcinogenic and mutagenic properties. Focus on PAH analogues such as azaheterocyclics and oxygenated PAHs has more recently been considered as well. Typical concentrations of PAHs in ambient atmospheric particles in Southern California are on the order of 0.04−2.5 ng m$^{-3}$ while the aza and oxo analogues are present at lower concentrations of 0.02−1.4 ng m$^{-3}$.[25] Table 1 lists the PAHs and analogues that have been analyzed as standards using ATOFMS, as well as their molecular weights and CAS registry numbers.

(21) Gard, E.; Mayer, J. E.; Morrical, B. D.; Dienes, T.; Fergenson, D. P.; Prather, K. A. *Anal. Chem.* **1997**, *69*, 4083−4091.
(22) Nordmeyer, T.; Prather, K. A. *Anal. Chem.* **1994**, *66*, 3540−3542.
(23) Prather, K. A.; Nordmeyer, T.; Salt, K. *Anal. Chem.* **1994**, *66*, 1403−1407.
(24) Salt, K.; Noble, C. A.; Prather, K. A. *Anal. Chem.* **1996**, *68*, 230−234.
(25) Schauer, J. J.; Rogge, W. F.; Hildemann, L. M.; Mazurek, M. A.; Cass, G. R.; Simoneit, B. R. T. *Atmos. Environ.* **1996**, *30*, 3837−3855.

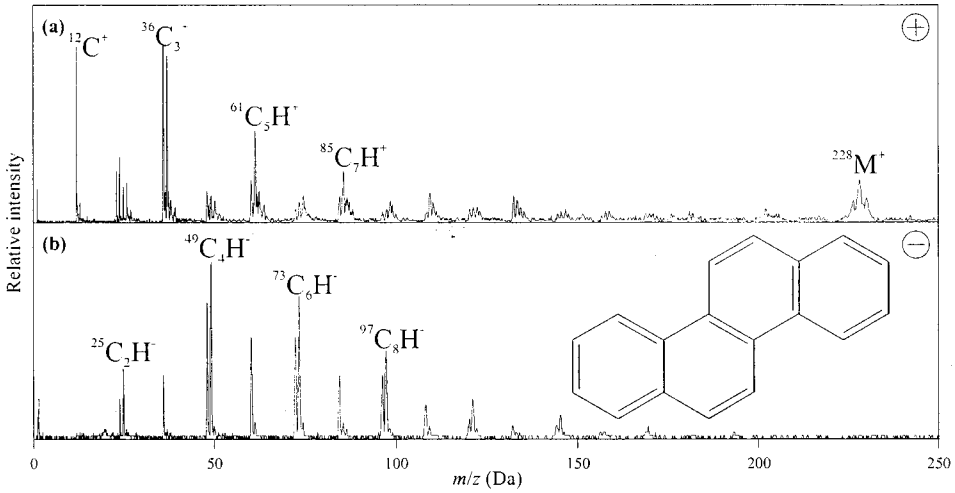


Figure 1. Positive and negative ion LDI mass spectra of chrysene.

The molar absorptivity ($\epsilon_o$) of PAHs and their heterocyclic analogues at 266 nm falls in the range of $10^3-10^5$, with larger ring systems such as chrysene exhibiting cross sections greater than $10^6$,[26] so it is expected that these compounds will be detected the most easily of all compounds using ATOFMS.

At low laser fluence, the base peak in the positive ion mass spectra of pure PAH particles is the parent ion ($M^{\bullet+}$) with very little fragmentation observed from these compounds. This is not unexpected since the ionization potential of most PAHs is relatively low (~7.5 eV for anthracene)[27] compared to many other organic compounds, and the resulting odd-electron ion is relatively stable, providing extremely low detection limits for these compounds.

At higher laser fluence, similar to that used for ambient and source testing experiments, considerable fragmentation is observed for the PAH compounds. Figure 1 shows the positive and negative ion mass spectra obtained from pure particles of chrysene. In the positive ion mass spectrum (Figure 1a), the parent ion signal at mass-to-charge ($m/z$) 228 is still significant. However, much larger signals are observed at low masses ($m/z$ <100). The base peak is observed at $m/z$ 36 $(C_3)^+$. Clusters of the type $(C_n)^+$ and $(C_nH)^+$ are commonly observed for the entire mass range from $n = 1$ up to the number of carbon atoms in each respective PAH. Clusters where $n$ is odd are favored over clusters where $n$ is even.

The negative ion mass spectrum shows similar fragmentation using both high and low laser fluence. In Figure 1b, the absence of any peaks in the parent ion region is apparent. The negative ion mass spectra of PAHs acquired with ATOFMS contrast previously published spectra obtained using LAMMA where $(M - H)^-$, $M^{\bullet-}$, and $(M + H)^-$ peaks are observed occasionally.[16] The base peak in the negative ion spectra of PAHs is typically observed at $m/z$ 25 $(HC{\equiv}C)^-$ or 49 $(HC{\equiv}CC{\equiv}C)^-$. Negative ion spectra previously published show that, even with 20-eV electron impact (EI), simple organic compounds readily undergo disintegration into carbon clusters ions $(C_n)^-$ and acetylide and polyacetylide ions $(C_nH)^-$, where $n$ is even.[28−30]

Panels a and b of Figure 2 show the positive and negative ion mass spectra of pure particles of phenathridine. Similar to the PAHs, phenanthridine yields a parent ion, $M^{\bullet+}$, at $m/z$ 179. Also observed in the high-mass region is a peak at $m/z$ 151, resulting from loss of HCN followed by loss of $H^{\bullet}$, similar to that observed from EI.[31] The base peak is observed at $m/z$ 39 $(C_3H_3)^+$. This and other low-mass ions observed correspond to the "low-" and "high"-aromatic series of peaks as identified by McLafferty and Turecek.[32] The low-aromatic series for electronegative substituents ($m/z$ 38, 39, 50, 51, 63, 64, 65, etc.), and the high-aromatic series for electron-donating substituents and heterocycles ($m/z$ 39, 40, 51, 52, 65, 66, 67, etc.) are major components of the mass spectra of aromatic compounds. The large amount of energy imparted to the sample in ATOFMS makes both series of peaks very intense in the mass spectra of most aromatic compounds.

The negative ion mass spectrum of phenanthridine is shown in Figure 2b. The base peak in the spectrum is observed at $m/z$ 26. Although this peak has been assigned to both $CN^-$ and $C_2H_2^-$ in much of the literature, during this study this peak has been observed dominantly in spectra of nitrogen-containing compounds and thus most likely can be attributed to $CN^-$. This result can be rationalized given the large difference in electron affinities of CN and $C_2H_2$, which are 3.8 and 0.5 eV, respectively.[33] In addition to $m/z$ 26, an entire series of nitrogen-containing cluster ions of the type $(C_nN)^-$ are observed at $m/z$ 50, 74, 98, and 122 (corresponding to odd numbers of carbon atoms). Also observed in the spectrum are carbon series $(C_n)^-$ and $(C_nH)^-$ peaks similar to the case of the PAHs.

(26) Valrose, T.; Stern, E. B.; Goncharova, A. A.; Messineva, N. A.; Trusova, N. V.; Efmkina, M. V. In *NIST Chemistry WebBook, NIST Standard Reference Database Number 69*; Mallard, W. G., Linstrom, P. J., Eds.; National Institute of Standards and Technology: Gaithersburg, MD, 1998; http://webbook.nist.gov.

(27) Franklin, J. L.; Haug, P. In *CRC Handbook of Chemistry and Physics*; Lide, D. R., Ed.; CRC Press: Boca Raton, FL, 1991; pp 10/213−10/219.

(28) Melton, C. E.; Rudolph, P. S. *J. Chem. Phys.* **1959**, *31*, 1485−1488.

(29) Aplin, R. T.; Budzikiewicz, H.; Djerassi, C. *J. Am. Chem. Soc.* **1965**, *87*, 3180−3186.

(30) Budzikiewicz, H. *Angew. Chem., Int. Ed. Engl.* **1982**, *15*, 482−493.

(31) Stein, S. E. In *NIST Chemistry WebBook, NIST Standard Reference Database Number 69*; Mallard, W. G., Linstrom, P. J., Eds.; National Institute of Standards and Tchnology: Gathersburg, MD, 1998; http://webbook.nist.gov.

(32) McLafferty, F. W.; Turecek, F. *Interpretation of Mass Spectra*, 4th ed.; University Science Books: Sausalito, CA, 1993.

(33) Miller, T. M. In *CRC Handbook of Chemistry and Physics*; Lide, D. R., Ed.; CRC Press: Boca Raton, FL, 1991; pp 10/180−10/193.

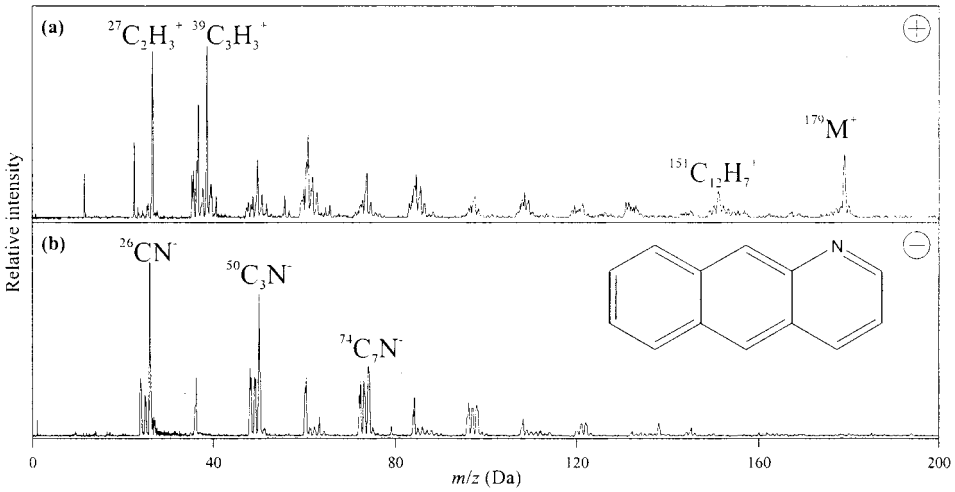


Figure 2. Positive and negative ion LDI mass spectra of phenanthridine.

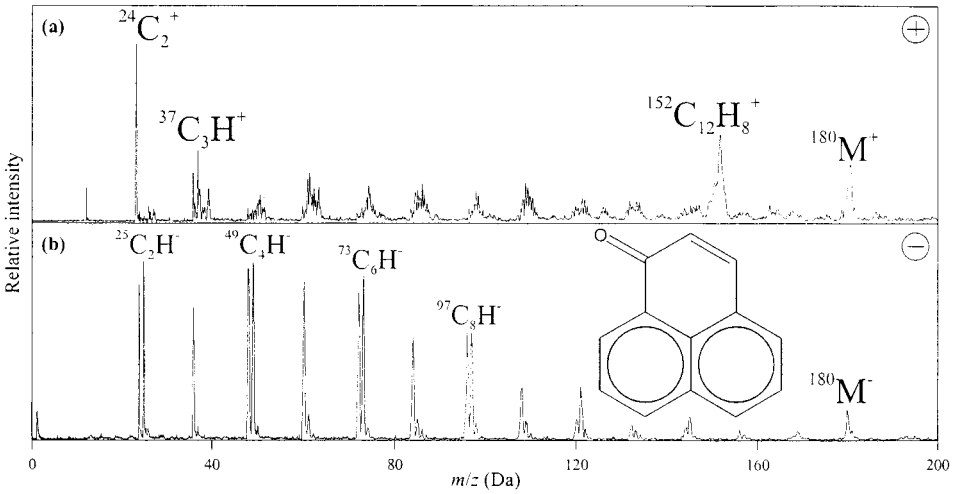


Figure 3. Positive and negative ion LDI mass spectra of perinaphthenone.

A number of oxygenated PAHs were characterized using ATOFMS. Positive and negative ion spectra for perinaphthenone are displayed in Figure 3. In the positive ion spectrum, the parent ion at $m/z$ 180 is observed. All oxygenated PAHs produced a small parent ion when sampled as pure particles. Most other peaks observed in the positive ion spectra of oxygenated PAHs are low-mass fragments ($m/z$ <100) due mostly to the "low"-aromatic series, with some peaks present due to the "high"-aromatic species common with heterocylic compounds. The base peak in these spectra is typically present at a low-mass carbon or carbon−hydrogen cluster ions such as $m/z$ 24 $(C_2)^+$ or 39 $(C_3H_3)^+$.

The negative ion spectra of all PAH ketones contain a small parent ion due to electron attachment at $(M^{\bullet -})$, such as shown in Figure 3b. This contrasts previous studies with LAMMA, where deprotonation to form the $(M - H)^-$ ion dominates.[16] One hydroxylated PAH (1,5-dihydroxynaphthalene, molecular weight 160) was studied, and in this case, deprotonation did occur, yielding peaks at both $m/z$ 158 and 159, corresponding to loss of one or both alcohol protons. Other than these parent ions, the only major peaks observed in the spectra consistently are due to the $(C_n)^-$ and $(C_nH)^-$ series. In some spectra, especially from 1,5-dihydroxynaphthalene, a small peak at $m/z$ 41 $(C_2HO)^-$ is observed.

**2. Aromatic and Functionalized Aromatic Hydrocarbons.** A large variety of smaller aromatic and functionalized aromatic compounds may be found in atmospheric particulate matter. Table 2 lists monocyclic aromatic compounds and derivatives that have been characterized with ATOFMS. Aromatic hydrocarbons exhibit mass spectra that are, in general, similar to the PAHs. A strong parent ion $(M^+)$ is observed, with major fragments from the loss of alkyl groups attached to the ring system. Large peak intensities are observed for low-mass carbon fragment ions, similar to PAHs.

Figures 4 and 5 show mass spectra obtained using ATOFMS analysis of functionalized aromatic compounds relevant to ambient particulate matter. In Figure 4, the positive and negative ion mass spectra of 1,3-dihydroxybenzene (resorcinol) are displayed. In the positive ion mass spectrum, a fairly large parent ion is observed at $m/z$ 110. Disregarding contaminant peaks at $m/z$ 18 and 23 ($NH_4^+/H_2O^+$ and $Na^+$, respectively), the remainder of the low-mass peaks very strongly resemble the relative intensities of the typical EI spectrum of this compound, with clusters of peaks centered around $m/z$ 27 $(C_2H_3^+)$, 39 $(C_3H_3^+)$, and 53 $(C_4H_5^+)$. The negative ion mass spectrum of resorcinol shows a very intense peak due to the deprotonated parent ion at $m/z$ 109. Carbon cluster ions ($C_n^-$ and $C_nH^-$) extend up to $m/z$ 121, suggesting that some carbon cluster formation does occur after desorption/

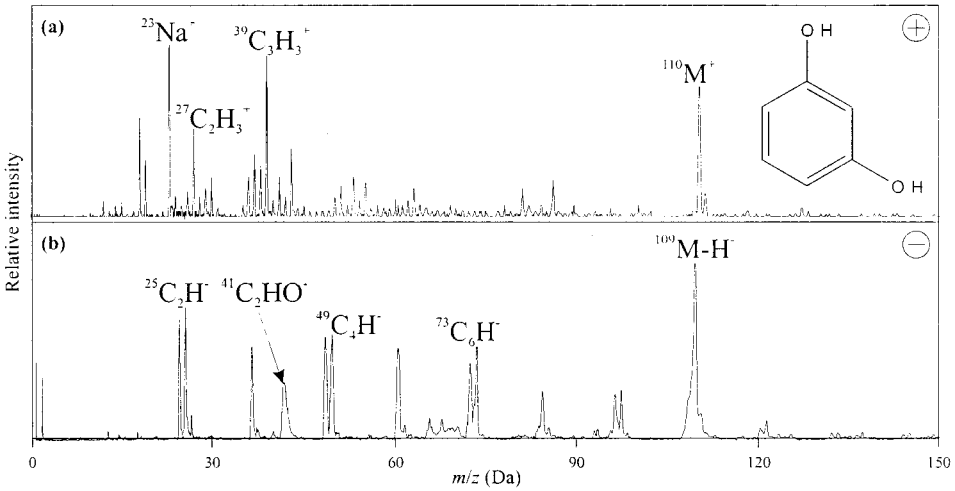


Figure 4. Positive and negative ion LDI mass spectra of 1,3-dihydroxybenzene.

Table 2. Aromatic Hydrocarbons and Functionalized Aromatics Analyzed Using ATOFMS

| compound | MW | CAS registry no. |
|---|---|---|
| 1,3-dihydroxybenzene | 110 | 108−46−3 |
| 4-cyanophenol | 119 | 767-00-0 |
| 2,4-dimethylphenol | 122 | 105-67-9 |
| 2,5-dimethylphenol | 122 | 95-87-4 |
| 3-pyridinecarboxylic acid | 123 | 59-67-6 |
| pyrazinecarboxamide | 123 | 98-96-4 |
| 1,2,4,5-tetramethylbenzene | 134 | 25619-60-7 |
| 4-nitrophenol | 139 | 100-02-7 |
| pentamethylbenzene | 148 | 700-12-9 |
| 1,7,7-trimethylbicyclo[2.2.1]-2-heptanone | 152 | 76-22-2 |
| 4-hydroxy-3-methoxybenzaldehyde | 152 | 121-33-5 |
| 2,4-dihydroxybenzoic acid | 154 | 89-86-1 |
| 1,2-benzenedicarboxylic acid | 166 | 88-99-3 |
| 2,6-pyridinedicarboxylic acid | 167 | 499-83-2 |
| 4-bromoaniline | 172 | 106-40-1 |
| *trans*-stilbene | 180 | 103-30-0 |
| 1,3,5-trichlorobenzene | 180 | 108-70-3 |
| 4-hydroxy-3,5-dimethoxybenzaldehyde | 182 | 134-96-3 |
| 2,4-diaminophenol dihydrochloride | 197 | 137-09-7 |
| phenylbenzoate | 198 | 93-99-2 |
| 2,4-dinitroanisole | 198 | 119-27-7 |
| 3,4,5-trimethoxybenzoic acid | 212 | 118-41-2 |
| triphenylphosphine | 262 | 603-35-0 |
| 1,3,5-tribromobenzene | 315 | 626-39-1 |

ionization since the molecule consists of only six carbon atoms. Other than these cluster ions, the only other fragment observed is $m/z$ 41 ($C_2HO^-$).

In Figure 5, the positive and negative ion mass spectra for 1,2-benzenedicarboxylic acid (phthalic acid) are shown. This compound is typically detected in atmospheric particles using traditional sampling and analysis techniques[25] and has recently been proposed as a tracer for secondary organic aerosol production.[34] In the positive ion mass spectrum, a peak at $m/z$ 167 denotes the presence of the even-electron protonated parent ion. A large peak at $m/z$ 149 corresponds to the loss of water from the protonated parent molecule. This peak, in addition to peaks at $m/z$ 39 ($C_3H_3^+$), 51 ($C_4H_3^+$), 65 ($C_5H_5^+$), and 105 ($C_7H_5O^+$), are all shifted higher by one mass unit in comparison to the EI mass spectrum of this compound. In addition, a peak at $m/z$ 121 ($C_7H_5O_2^+$) is observed that does not occur in the EI mass spectrum. This peak probably results from the loss of $H_2O$ and CO from the protonated parent molecule, which cannot occur in EI because of the lack of a protonated parent ion. In the negative ion mass spectrum, a deprotonated parent ion is observed at $m/z$ 165. Fragments from the consecutive loss of two $CO_2$ molecules are observed at $m/z$ 121 ($C_7H_5O_2^-$) and 77 ($C_6H_5^-$). Other prominent peaks observed are due to the carbon clusters ($C_n^-$) and ($C_nH^-$).

**3. Aliphatic Hydrocarbons and Derivatives.** Long-chain aliphatic hydrocarbons and their aldehyde, ketone, alcohol, and acid derivatives are commonly found in atmospheric particulate matter in both urban and rural locations because they are emitted from both anthropogenic and natural sources.[35−38] In addition to long-chain species, a number of smaller aliphatic compounds are also found in atmospheric particles. Dicarboxylic acids containing 2−9 carbon atoms are routinely detected in airborne particles at concentrations from $10^1$ to $10^3$ ng $m^{-3}$ [25,39] and are believed to be produced from both primary sources[40] and secondary aerosol chemistry.[41] Polyfunctional aliphatic compounds such as amino acids and polyols have recently been proposed as a contributors to water-soluble organic carbon in the atmosphere,[42] but studies of their presence[43,44] are rare at this point. Table 3 lists the aliphatic compounds that have been studied using ATOFMS.

Figure 6 shows the positive and negative ion mass spectra of nonanal acquired using ATOFMS. Nonanal is one of the more common aldehydes present in atmospheric particles and has been used as a tracer for particles of meat cooking.[25] The positive ion

(34) Schauer, J. J. California Institute of Technology, Pasadena, CA, 1998.

(35) Rogge, W. F.; Hildemann, L. M.; Mazurek, M. A.; Cass, G. R.; Simoneit, B. R. T. *Environ. Sci. Technol.* **1993**, *27*, 636−651.
(36) Rogge, W. F.; Hildemann, L. M.; Mazurek, M. A.; Cass, G. R.; Simoneit, B. R. T. *Environ. Sci. Technol.* **1993**, *27*, 1892−1904.
(37) Rogge, W. F.; Hildemann, L. M.; Mazurek, M. A.; Cass, G. R.; Simoneit, B. R. T. *Environ. Sci. Technol.* **1993**, *27*, 2700−2711.
(38) Rogge, W. F.; Hildemann, L. M.; Mazurek, M. A.; Cass, G. R.; Simoneit, B. R. T. *Environ. Sci. Technol.* **1994**, *28*, 1375−1388.
(39) Sempere, R.; Kawamura, K. *Atmos. Environ.* **1994**, *28*, 449−459.
(40) Kawamura, K.; Kaplan, I. R. *Environ. Sci. Technol.* **1987**, *21*, 105−110.
(41) Grosjean, D.; Friedlander, S. K. *Adv. Environ. Sci. Technol.* **1980**, *9*, 435−473.
(42) Saxena, P.; Hildemann, L. M. *J. Atmos. Chem.* **1996**, *24*, 57−109.
(43) Gorzelska, K.; Galloway, J. N. *Global Biogeochem. Cycles* **1990**, *4*, 309−333.
(44) Dod, R. L.; Gundel, L. A.; Benner, W. H.; Novakov, T. *Sci. Total Environ.* **1984**, *36*, 277−282.

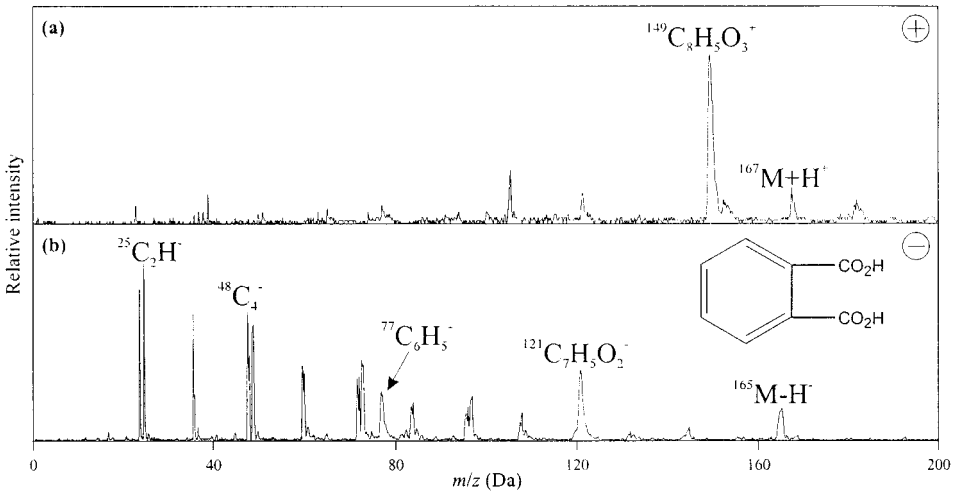


Figure 5. Positive and negative ion LDI mass spectra of 1,2-benzenedicarboxylic acid.

Table 3. Aliphatic and Functionalized Aliphatics Analyzed Using ATOFMS

| compound | MW | CAS registry no. |
|---|---|---|
| urea | 60 | 57-136 |
| glycine | 75 | 56-40-6 |
| thioacetamide | 75 | 62-55-5 |
| methanesulfonic acid | 96 | 75-75-2 |
| *cis*-2-butenedioic acid | 116 | 110-16-7 |
| diethylaminoethanol | 117 | 100-37-8 |
| butanedioic acid | 118 | 110-15-6 |
| oxalic acid dihydrate | 126 | 6153-56-6 |
| pentanedioic acid | 134 | 110-94-1 |
| 1-nonanal | 142 | 124-19-6 |
| camphor | 152 | 76-22-2 |
| 1,6-anhydro-$\beta$-D-glucopyranose | 162 | 498-07-7 |
| l-arginine | 174 | 74-79-3 |
| 1-hexadecanol | 242 | 36653-82-4 |
| 1-hexadecanoic acid | 256 | 57-10-3 |
| *cis*-9-octadecenoic acid | 282 | 112-80-1 |
| methyl octadecanoate | 298 | 112-61-8 |
| 1-docosanol | 326 | 661-19-8 |
| 5$\alpha$-cholestane | 372 | 481-21-0 |
| cholesterol | 386 | 57-88-5 |
| *n*-octacosane | 394 | 630-02-4 |
| hexadecylhexadecanoate | 480 | 540-10-3 |

mass spectrum contains almost no information indicative of molecular composition. Even at low laser fluence, only low-mass carbon cluster fragments are observed. The ($C_nH_{2n+1}CO^+$) series typically used to identify carbonyl compounds in EI mass spectrometry[32] is of little diagnostic value because this series is not observed above $C_5$ in the typical nonanal spectra. Carbon clusters ($C_n^-$ and $C_nH^-$) are observed in the negative ion mass spectrum, as with all other organic compounds analyzed. A small deprotonated ion is indicated by the peak at $m/z$ 141. The only other distinct peak in the spectrum is observed at $m/z$ 45 and is presumably due to ($C_2H_5O^-$).

Nonanal is the only long-chain aliphatic compound studied for which ions were detected using ATOFMS. For the other long-chain species studied (1-hexadecanol, 1-hexadecanoic acid, oleic acid, docosanol, octacosane, hexadecyl hexadecanoate), no ions were detected using either positive or negative polarities, other than contaminant metal cations and oxoanions. This is not surprising given that most long-chain aliphatic compounds exhibit relatively small molar absorptivities at 266 nm; i.e., the $C_{10}$ analogue to nonanal, decanal, has $\epsilon_o \sim 16$.[26] Therefore, unless other compounds are present in the particles that can act as a matrix similar to matrix-assisted laser desorption/ionization (MALDI), it is unlikely that these compounds can be detected with the required sensitivity using 266-nm radiation. In fact, some of these long-chain compounds have been detected in some recent source characterization experiments,[45] indicating that under certain circumstances, matrix effects do in fact allow for detection of these compounds in real samples.

In Figure 7, the positive and negative ion mass spectra of glycine acquired using ATOFMS are displayed. A strong protonated parent ion is observed at $m/z$ 76. Similar to the EI mass spectrum, $m/z$ 30 ($CH_4N^+$) is the base peak. Other major fragments observed are present at $m/z$ 27 ($C_2H_3^+$), 32 ($CH_6N^+$), and 45 ($CHO_2^+$). The presence of sodium contaminant at $m/z$ 23 ($Na^+$) also results in adduct formation of a sodiated parent ion at $m/z$ 98 $(M + Na)^+$. The negative ion mass spectrum consists of a deprotonated parent ion at $m/z$ 74 and fragments at $m/z$ 26 ($CN^-$), 42 ($C_2H_2O^-$), and 45 ($CHO_2^-$).

In general, polyfunctional aliphatic compounds ionize easier and can be detected with greater sensitivity than long-chain species. Formation of protonated molecules greatly aids in the identification of these compounds by limiting their fragmentation to fairly simple mechanisms (loss of $H_2O$, $CO_2$, etc.) In addition, the information available in the negative ion mass spectra should not be overlooked, since the presence of oxygen and nitrogen in the molecule can be observed. In some cases, such as nonanal, it is observed that detection and identification cannot be performed with positive ions and must be discerned from negative ion mass spectra. Similar observations were recently reported for 1,6-anhydro-$\beta$-D-glucopyranose (levoglucosan) in biomass burning particles.[46]

**4. Organic Salts.** The presence of elevated concentrations of nitric and sulfuric acid and ammonia in the gas phase in the atmosphere allows for the possible reaction of these compounds with existing organic compounds to form salts that can be either

(45) Silva, P. J.; Suess, D. T.; Prather, K. A., manuscript in progress.
(46) Silva, P. J.; Liu, D.-Y.; Noble, C. A.; Prather, K. A. *Environ. Sci. Technol.* **1999**, *33*, 3068−3076.

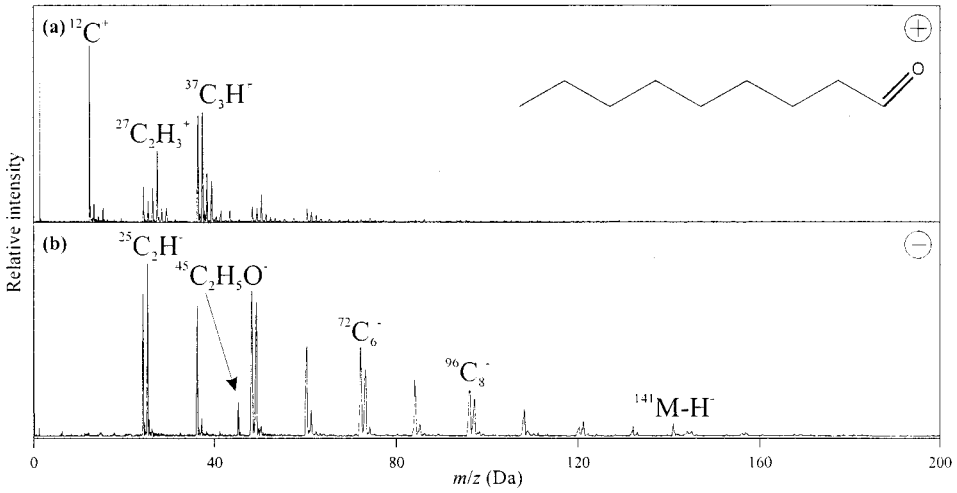


Figure 6. Positive and negative ion LDI mass spectra of *n*-nonanal.

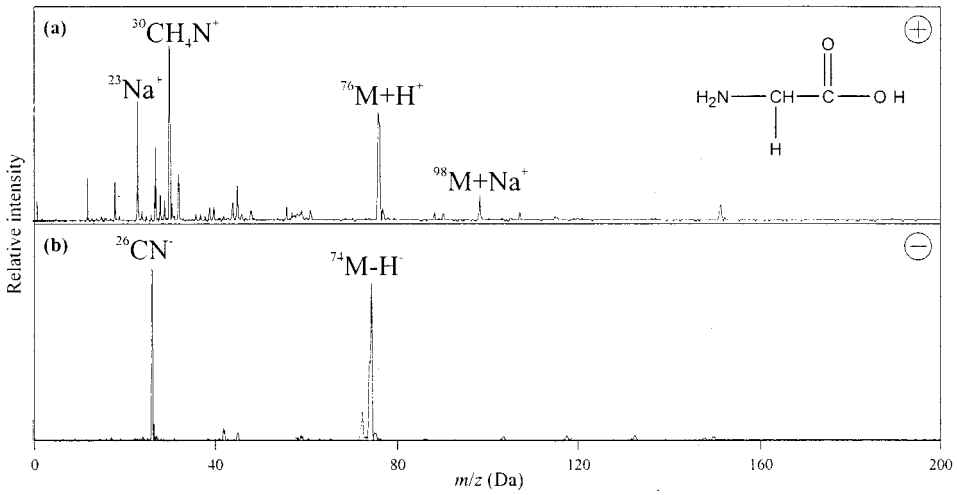


Figure 7. Positive and negative ion LDI mass spectra of glycine.

Table 4. Organic Salts Analyzed Using ATOFMS

| compound | MW | CAS registry no. |
|---|---|---|
| acetic acid, ammonium salt | 77 | 631-61-8 |
| methanesulfonic acid, ammonium salt | 113 | 22515-76-0 |
| methanesulfonic acid, sodium salt | 118 | 2386-57-4 |
| triethylamine, nitrate salt | 164 | 27096-31-7 |
| diethylethanolamine, nitrate salt | 180 | n/a |

volatile or semivolatile. For instance, amines are present in the gas phase in the atmosphere due to emissions from livestock[47] and can react with acids to form salts analogous to ammonia-acid reactions (see Table 4).[48]

Figure 8 shows the positive and negative ion mass spectra of a quarternary ammonium salt, diethylethanolamine nitrate. These particles were generated by reaction of diethylethanolamine with nitric acid in the gas phase. The positive ion mass spectrum shows an ion due to the intact quaternary ammonium cation at $m/z$ 118. A fragment at $m/z$ 102 is probably due to loss of $CH_3^\bullet$ from the parent ion. An intense peak at $m/z$ 86 ($C_5H_{12}N^+$) results from the α cleavage of $^\bullet CH_2OH$ and is characteristic of quaternary ammonium compounds with ethyl substituents. Four major peaks are observed in the negative ion mass spectrum. Mass-to-charge 46, 62, and 125 are nitrate-related peaks, assigned to ($NO_2^-$), ($NO_3^-$), and ($HNO_6^-$), respectively. The peak at $m/z$ 97 is probably due to $HSO_4^-$ contamination. The lack of peaks due to carbon clusters in the negative ion mass spectra is striking compared to all the previous spectra. This indicates that, for quaternary ammonium salts, the cation is desorbed as an intact cation, making the classification of the particle as "organic" impossible with the negative ion mass spectrum alone. This illustrates the importance of obtaining both positive and negative ion mass spectra when studies of particles of unknown composition are performed.

In Figure 9, the positive ion and negative mass spectra of sodium methanesulfonate are displayed. Methanesulfonic acid (MSA) and its sodium and ammonium salts are of interest as a source of non-sea salt sulfate.[49,50] With this compound, large signals due to methanesulfonate anion and fragments are observed

(47) Mosier, A. R.; Andre, C. E.; Viets, F. G., Jr. *Environ. Sci. Technol.* **1973**, *7*, 642−644.

(48) Seinfeld, J. H.; Pandis, S. N. *Atmospheric Chemistry and Physics: From Air Pollution to Climate Change*; John Wiley & Sons: New York, 1998.

(49) Huebert, B. J.; Zhuang, L.; Howell, S.; Noone, K.; Noone, B. *J. Geophys. Res.* **1996**, *101*, 4413−4423.

(50) Bates, T. S.; Calhoun, J. A.; Quinn, P. K. *J. Geophys. Res.* **1992**, *97*, 9859−9865.

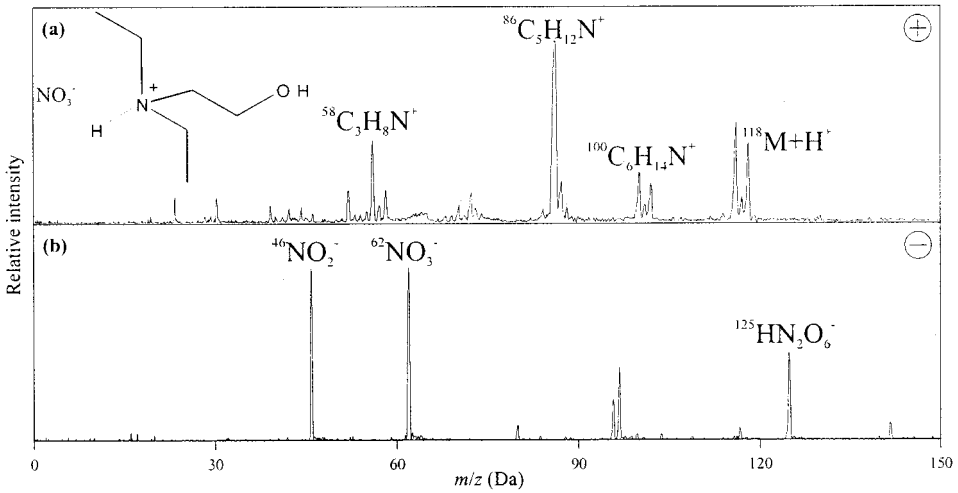


Figure 8. Positive and negative ion LDI mass spectra of diethylethanolammonium nitrate.

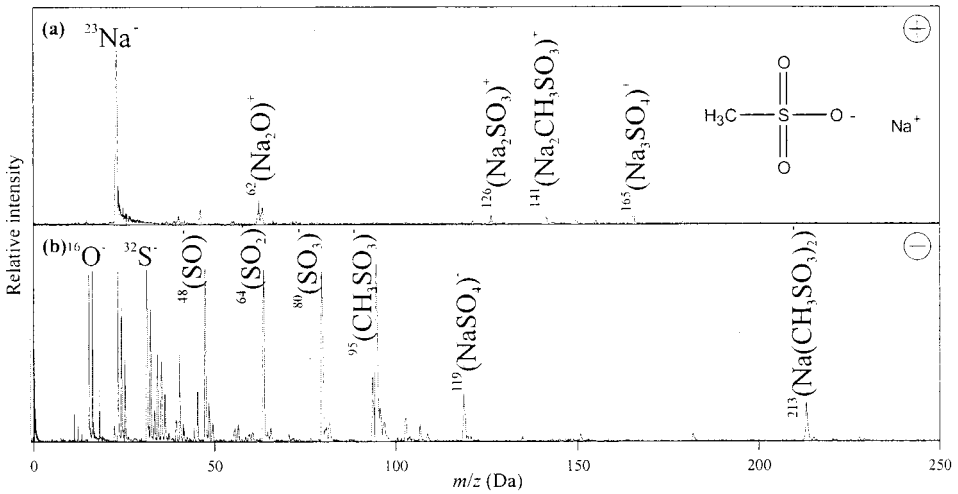


Figure 9. Positive and negative ion LDI mass spectra of sodium methanesulfonate.

in the negative ion mass spectrum, while only sodium and cluster ions are observed in the positive ion mass spectrum. Interestingly, the ammonium salt of this compound gave only atomic cations in the positive ion mass spectrum ($H^+$, $C^+$, $N^+$, $O^+$, $S^+$) and yielded no negative ions, indicating just how large an influence a small change in matrix can make on the mass spectra. Particle mass spectra resembling both standards (ammonium and sodium methanesulfonate) have been observed in ambient mass spectra collected in Riverside.

**5. Potential Application of Results to Ambient Particles.** In the atmosphere, particles consist of a complex mixture of a range of organic compounds, in addition to a full array of inorganic species. This can constrain the interpretation of organic mass spectra because only one mass spectrum is acquired for a particle containing perhaps hundreds of compounds. In addition, the presence of certain compounds can serve as a matrix which may change the detection characteristics of other compounds. As an example, Figure 10 shows the positive and negative ion mass spectra of particles containing a 1:1 mixture of resorcinol (Figure 4) and phthalic acid (Figure 5). In contrast to Figure 4, where a parent ion and fragments are observed from resorcinol, the presence of acidic protons from phthalic acid results in an intense even-electron protonated parent ion for resorcinol at $m/z$ 111. This peak is much more intense than the protonated parent observed for phthalic acid at $m/z$ 167. A smaller peak at $m/z$ 110 from the loss of an electron in resorcinol is still observed as well. In the presence of a proton source such as phthalic acid, compounds that have polar functional groups containing oxygen and nitrogen can form adduct ions. Even oxygenated PAHs such as perinaphthenone (shown pure in Figure 3) show evidence for some proton attachment in the presence of an acid.

Although the interpretation of organic compounds in single-particle mass spectra can be difficult, several strategies can be used depending on the goal of the analysis. Being able to characterize particles simply based on functional group information would represent a major advancement in particulate matter analysis, compared to current procedures that identify only total organic carbon, assuming a constant amount of oxygen- and nitrogen-containing organic compounds. In this case, negative ion mass spectra are extremely useful for identifying particles that contain solely hydrocarbons versus particles that include functionalized compounds. Although some recent work has focused on using Fourier transform infrared spectroscopy (FT-IR) for functional group information,[51,52] this has involved samples collected on filters, and a single-particle approach would be desirable.

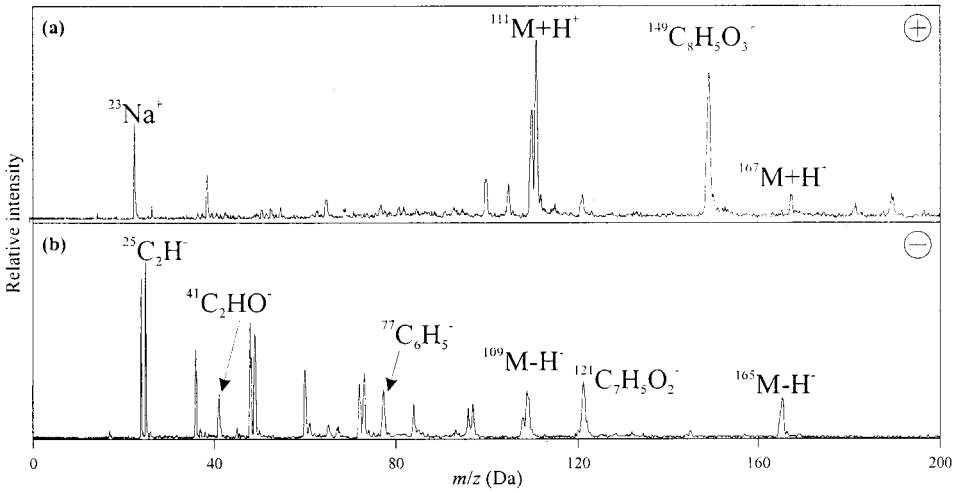


Figure 10. Positive and negative ion LDI mass spectra of a 1:1 mixture of 1,3-dihydroxybenzene and 1,2-benzenedicarboxylic acid.

The tendency of negative ions to undergo disintegration, though making molecular identification more difficult, actually aids in determining the presence of functional group information. The presence of a peak at $m/z$ 26 is due to $CN^-$, a definitive marker for species with carbon−nitrogen bonds in the particle. The presence of a series of peaks of the type $C_nN^-$, where $n$ is odd ($m/z$ 26, 50, 74, 90, etc.) indicates the presence of organic nitrogen atoms since only $CN^-$ by itself can be due to the cyanide ion. Phosphorus-containing compounds display a similar series of peaks due to the analogous series $C_nP^-$ ($m/z$ 43, 67, 91, etc.)

Several different oxygen-containing fragments in negative ion mass spectra may be used to identify particles containing oxygenated species. A peak present at $m/z$ 41 ($C_2HO^-$) is nearly ubiquitous in the spectra of compounds containing alcohol functionality. A second possible marker is the peak that occurs at $m/z$ 45 due to two different oxygen-containing fragments, $CHO_2^-$ and $C_2H_5O^-$. Although certain positive ions can also be indicative of oxygen species, e.g., $m/z$ 43 ($C_2H_3O^+$), negative ions do not suffer from as many interferences from ions of the same nominal mass; e.g., $m/z$ 43 can also be $C_3H_7^+$ or $C_2H_5N^+$.

Several other fragment ions in negative ion mass spectra merit special attention. Mass-to-charge 42 ($CNO^-$ or $C_2H_2O^-$) is a peak observed quite often in source emissions experiments and ambient data acquisition.[1,45] This peak seems to be due dominantly to $CNO^-$, identifies the presence of an amide functional group, and does not arise from the desorption/ionization process itself, at least for the limited number of species studied here. Although this peak was observed in the negative ion mass spectrum of glycine (Figure 7), it can easily be attributed to $C_2H_2O^-$ in this case. The peak has not been observed from any other compound that has nitrogen and oxygen functional groups in its structure, except when an actual amide group is present. While not quite as common as the previously mentioned peaks, $m/z$ 93 ($C_6H_5O^-$) can be an important peak for identifying particles containing oxygenated aromatic compounds. However, at this higher mass, there are more interferences from ions of the same nominal mass and caution must be exercised in assigning the peak to this ion.

Analysis of negative ion mass spectra also has disadvantages in certain areas. Negative ion mass spectra, although helpful for determining heteroatoms present in organic particles, are not as useful for distinguishing organic carbon (OC) from black or elemental carbon (EC). In this case, the tendency of many organic compounds to disintegrate into carbon cluster-type ions, $C_n^-$ and $C_nH^-$, implies that EC/OC determinations from negative ion mass spectra alone are highly uncertain. Further work is being performed to see if this holds true with the presence of complex mixtures present in the atmosphere. Previous work with LAMMA concluded that it is far more precise to use positive ion mass spectra for this purpose,[53] where traditional fragmentation mechanisms dominate.

Halogenated organic compounds can also be difficult to identify using data from negative ions. Although fluorine-, chlorine-, and bromine-containing organic compounds yield large atomic anions due to the halogen species, it is impossible to discern them from inorganic halides present in the particle. In the positive ion mass spectra, carbon−halogen cluster ions can be observed at $m/z$ 31 ($CF^+$), 47 and 49 ($CCl^+$), and 91 and 93 ($CBr^+$). These cluster ions are more typically observed with high laser fluence. Chlorine and bromine can be identified on the basis of isotope ratios and are observed from aromatic compounds with halogen functional groups (See Table 2). The fluorine peak was observed from the presence of particles containing fluorocarbons similar to previous reports.[54]

A number of positive ions can potentially be used to obtain chemical structure information. Because of the high energy imparted to the sample using laser desorption/ionization, small mass fragments are typically quite large in ion intensity. The high- and low-aromatic series of peaks are frequently present. However, the large energy used on the sample can also make these two series hard to distinguish as the relative intensities do not match those obtained from EI mass spectrometry. However, the presence of alkyl groups can be observed similar to EI mass spectrometry. Although the detection of long-chain alkanes is unlikely with the use of 266-nm radiation, the series of alkyl fragments ($m/z$ 15, 29, 43, 57, etc.) can be used to identify alkyl substituents. Mass-

(51) Pickel, T.; Allen, D. T.; Pratinsis, S. E. *Atmos. Environ.* **1990**, *24A*, 2221−2228.
(52) Blando, J. D.; Porcja, R. J.; Li, T.-H.; Bowman, D.; Lioy, P. J.; Turpin, B. J. *Environ. Sci. Technol.* **1998**, *32*, 604−613.
(53) Mauney, T.; Adams, F. *Sci. Total Environ.* **1984**, *36*, 215−224.
(54) Schelles, W.; Van Grieken, R. *Anal. Chem.* **1997**, *69*, 2931−2934.

to-charge 15 and 29 in particular are readily observed from compounds with methyl and ethyl substituents.

Several peaks in positive ion mass spectra that can also provide information on heteroatoms in organic molecules are $m/z$ 31 ($CH_3O^+$), which is a peak that arises from oxygenated organic compounds. Mass-to-charge 31 can also be due to $CF^+$ in particles consisting of fluorine-containing organic compounds. Another important peak observed is $m/z$ 32 ($S^+$). Although a limited number of sulfur-containing compounds were characterized in this study, no non-sulfur-containing compounds produced ions of this mass, while all sulfur compounds did.

The exclusive use of only positive ion or negative ions mass spectra inherently limits the ability to interpret mass spectra containing components from organic compounds. The abundant and diverse number of compounds present in the atmosphere, from PAHs to multiply substituted polar compounds, dictates that dual-polarity ion acquisition is necessary to obtain as much information as possible. Two research groups, including our own, have constructed instrumentation for dual-polarity data acquisition,[2,21] and data from these have proven useful for inorganic composition analysis.[2,8] But data from this study indicate that dual-ion information should also be extremely helpful for analysis of organic compounds.

The detection of several specific classes of organic compounds is enhanced greatly by dual-polarity ion analysis. One very practical application for dual-ion analysis is for the detection of organic acids. All organic acids studied yield protonated positive parent ions and deprotonated negative parent ions in the mass spectra (Figures 6, 9, and 10). This is advantageous since resolution in time-of-flight mass spectrometers used for particle analysis is typically 500−1000. With a protonated peak in the positive ion mass spectrum and a deprotonated peak in the negative ion mass spectrum, one can potentially identify the peak as due to parent ions given the two mass unit difference between the parent ion in the positive and negative ion mass spectra.

A second very important application for dual-ion data analysis is for organic salts. As observed in Figure 8, no negative ion carbon clusters are observed from the analysis of some organic salts. This is useful information, since all neutral organic compounds analyzed using ATOFMS have been observed to give these clusters. The use of dual-ion data acquisition thus provides an important capability for identifying organic salts based on the lack of correlating organic fragments in the other polarity spectrum. The lack of carbon clusters in a negative ion mass spectrum that is correlated with a positive ion mass spectrum containing organic fragments strongly indicates the presence of organic salts rather than neutral organic compounds.

## CONCLUSIONS

Positive ion mass spectra acquired using ATOFMS are qualitatively similar to data acquired using standard EI-MS techniques for hydrocarbon compounds. For species with polar functional groups, formation of protonated molecular ions plays a significant role. This is especially true in the case of organic acids, whose spectra typically exhibit fragments that are shifted up by one $m/z$ unit from the fragments typical in EI mass spectra. Negative ion mass spectra are dominated by the presence of carbon cluster ions and simple polyatomic heteroatoms that can be very useful for distinguishing particles containing only nonpolar compounds from those including polar compounds. Acquisition of dual-polarity mass spectra greatly helps with interpreting the data on organic compounds. This is the first work to focus on the use of single-particle laser desorption/ionization mass spectrometry for the analysis of organic compounds. Further work is necessary to fully understand ion formation mechanisms, especially from complex samples. However, this broad-scope study is the first step toward being able to detect differences in the organic composition of particles and establish tracers for classes of organic compounds.

## ACKNOWLEDGMENT

The authors thank Professor Glen Cass, Dr. Jamie Shauer, and the rest of the Cass research group from the Environmental Engineering Department at the California Institute of Technology for advice in choosing standards and for providing some chemicals. This research was supported by Grant CHE-9412317 from the National Science Foundation and completed with help from EPA STAR Fellowship grant U915354.

Received for review October 4, 1999. Accepted May 12, 2000.

AC9910132